



1 **Rethinking the deployment of static chambers for CO₂ flux** 2 **measurement in dry desert soils**

3 Nadav Bekin, Nurit Agam

4 ¹Blaustein Institutes for Desert Research, Ben-Gurion University of the Negev, Sede-Boqer Campus, 84990, Israel

5 *Correspondence to:* Nurit Agam (agam@bgu.ac.il)

6 **Abstract.** The mechanisms underlying the soil CO₂ flux (F_s) in dry desert soils are not fully understood. To better
7 understand these processes, we must accurately estimate these small fluxes. The most commonly used method,
8 static chambers, inherently alter the conditions that affect the flux and may introduce errors of the same order of
9 magnitude as the flux itself. Regional and global assessments of annual soil respiration rates are based on
10 extrapolating point measurements conducted with flux chambers. Yet, studies conducted in desert ecosystems
11 rarely discuss potential errors associated with using static chambers in dry and bare soils. We hypothesized that a
12 main source of error is the collar protrusion above the soil surface. During the 2021 dry season, we deployed four
13 automated chambers on collars with different configurations in the Negev Desert, Israel. F_s exhibited a repetitive
14 diel cycle of nocturnal uptake and daytime efflux. CO₂ uptake measured over the conventionally protruding
15 collars was significantly lower than over the collars flushed with the soil surface. Using thermal imaging, we
16 proved that the protruding collar walls distorted the ambient heating and cooling regime of the topsoil layer,
17 increasing the mean surface temperatures. Higher soil temperatures during the night suppressed the flux driving
18 forces, i.e., soil-atmosphere CO₂ and temperature gradients, ultimately leading to an underestimation of up to
19 50% of the actual F_s. Accordingly, the total daily CO₂ uptake by the soil in the conventionally deployed collars
20 was underestimated by 35%. This suggests that desert soils are a larger carbon sink than previously reported and
21 that drylands, which cover approximately 40% of Earth's terrestrial surface, may play a significant role in the
22 global carbon balance.



23 1 Introduction

24 Soil respiration, i.e., the carbon dioxide (CO₂) efflux from the soil to the atmosphere, is among the largest
25 components of the carbon balance in terrestrial ecosystems, contributing approximately 60 PgC to the atmosphere
26 every year (Houghton, 2007). In arid and semi-arid environments, soil respiration is mostly considered to be
27 restricted to short pulses of increased moisture availability from rainfall events, during which microbial metabolic
28 activity increase rapidly, followed by long periods of desiccation and low to negligible soil respiration rates
29 (Austin et al., 2004; Cable et al., 2008). In the last two decades, studies carried out in several deserts have
30 challenged this paradigm, reporting a diel course of CO₂ exchange during dry periods, consisting of nocturnal
31 CO₂ uptake and daytime efflux (Sagi et al., 2021; Lopez-Canfin et al., 2022). Researchers usually attribute this
32 diel cycle to changes in soil temperatures and soil air pressure that leads to cycles of expansion/contraction of soil
33 air, following the ideal gas law (Yang et al., 2020). These cycles change the surface CO₂ concentration and may
34 generate a soil-atmosphere pressure gradient (Ganot et al., 2014), both driving forces for soil CO₂ flux (F_s).
35 Another explanation is based on Henry's Law. It states that diurnal fluctuations of soil temperatures change the
36 solubility of soil CO₂ in water films, which changes the concentration of gaseous CO₂ in soil pores, leading to the
37 exchange of CO₂ between the soil and the atmosphere by diffusion (Fa et al., 2016). In saline/alkaline soils, this
38 process is thought to cause a diel cycle of calcium carbonate (CaCO₃) precipitation/dissolution, which enhances
39 F_s (Hamerlynck et al., 2013; Fa et al., 2016). Yet, the factors controlling F_s in dry desert soils and the partitioning
40 between them are still under debate.

41 Furthermore, the ability to accurately estimate the soil CO₂ flux in desert soils at the very dry-end is controversial
42 due to the potential for measurement-induced modifications to soil and atmospheric conditions that can introduce
43 errors of the same order of magnitude as the flux being measured. This problem is exacerbated when using static
44 chambers to measure flux, as the chambers inherently alter the conditions that affect the flux (Pumpanen et al.,
45 2010 ; Parkin et al., 2012). During efflux, CO₂ concentration in the chamber builds up, decreasing the diffusion
46 gradient between CO₂ in the soil pores and the chamber headspace, thereby altering CO₂ concentration within the
47 top soil layer and reducing the flux (Pumpanen et al., 2004). Artificial changes in air pressure within the chamber
48 headspace compared to the ambient atmosphere are another source of error (Bain et al., 2005; Lund et al., 1999).

49 There are additional sources of errors associated with the chamber-soil contact method (Ngao et al., 2006; Baram
50 et al., 2022). Flux chambers are typically deployed on a collar (i.e., PVC pipe) that is inserted into the soil, with
51 the upper 3-5 cm of the collar protruding above the soil surface to allow for chamber deployment. This practice
52 modifies the soil surface temperature by shading a portion of the measured surface area. The non-representative
53 soil surface temperature results in modified heat exchange between the soil and the atmosphere, as well as a
54 modified soil temperature profile (Ninari and Berliner, 2002). Soil microbial and physical processes that drive F_s
55 are susceptible to changes in soil temperature (Cable et al., 2011), and thus shading the soil surface can lead to
56 errors in F_s measurements. While these effects are likely minimal in temperate, vegetated areas, they could be
57 significant in dry bare soil, partly because fluctuations in surface temperatures are not regulated by vegetation
58 cover as in humid environments. Desert soils also have lower specific heat capacity than soils in humid
59 environments due to lower water content (Hillel, 1998). The lower water content also means that a larger portion
60 of the available energy is invested in soil heating rather than stored as latent heat during evaporation (Brutsaert,
61 1982). However, studies using static chambers in desert ecosystems rarely discuss potential errors associated with



62 the unique characteristics of desert soils. Moreover, to our knowledge, the effect of collar height above the surface
63 on soil surface temperature and, consequently, on F_s was never studied.

64 Under dry soil conditions, the depth to which the collar is inserted can also significantly influence the flux
65 measurements. The ideal insertion depth is debatable, as both shallow and deep collar insertion depths can lead to
66 errors, depending on climate and soil conditions. Inserting the collar to a shallower depth than the depth to which
67 feedback from the chamber still affects gas concentrations may result in lateral diffusion, leading to
68 underestimation of the vertical flux (Healy et al., 1996). However, insertion depth of only 2.5 cm and a
69 measurement period of 10 minutes will reduce this underestimation to 1% for a soil with air-filled porosity of 0.3
70 $\text{m}^3 \text{m}^{-3}$ (Hutchinson and Livingston, 2001). Hence, for short measurement periods (common today) and soils with
71 low effective diffusivity, errors resulting from lateral diffusion may be insignificant. With current static chamber
72 systems, even small F_s measured in dry desert soils can be accurately quantified with much shorter measurement
73 periods of only 1-2 minutes (Yang et al., 2022), thus overcoming a significant drawback of the shallow collars.
74 Deep collar insertion, on the other hand, can lead to either overestimation or underestimation of the flux by
75 generating vertical mass flow of air along the collar walls or by facilitating root cutting, respectively (Heinemeyer
76 et al., 2011). Still, in most studies, collars are inserted to a depth of ~5-10 cm into the soil and, in some cases, to
77 a depth of 30-60 cm, while more than a third of all authors fail to report the collar insertion depth (Rochette and
78 Eriksen-Hamel, 2008; Cable et al., 2011; Fa et al., 2018; Jian et al., 2020; Sagi et al., 2021; Yang et al., 2022).

79 In this paper, we aimed to investigate the effect of collar height above the soil surface and collar depth of insertion
80 on F_s in a dry bare desert soil. Given the small fluxes in these conditions, and the fact that regional and global
81 assessments of annual soil respiration are based on extrapolating point measurements conducted with flux
82 chambers (Jian et al., 2020), minimizing measurement errors associated with the collar deployment technic is
83 critical. Arid and semi-arid regions, which comprise approximately 40% of earth's terrestrial surface, constitute
84 the largest uncertainty on mean annual soil respiration estimations (Stell et al., 2021). Improving the accuracy of
85 F_s measurements in desert environments is essential for enhancing our understanding of the terrestrial carbon
86 balance and our ability to predict climate change.

87 **2 Materials and Methods**

88 **2.1 Research site**

89 The study was carried out at the Wadi Mashash Experimental farm in the Northern Negev, Israel (31°04'14''N,
90 34°51'62''E; 360 m.a.s.l; 65 km SE of the Mediterranean Sea). The climate in the research site is arid, with an
91 average annual rainfall of 116 mm (IMS, 2021), occurring between October and April. The daily mean maximum
92 and minimum temperatures for January (winter) are 15.9 C° and 8.0 C°, respectively, while those for August
93 (summer) are 33.3 C° and 20.7 C°. During the summer season, the prevailing wind direction is NW due to the sea
94 breeze carrying water vapor from the Mediterranean Sea inland. The sea breeze reaches its peak at a wind speed
95 of 7 m s^{-1} (at 10 m height) in the afternoon. The research is located on a largely bare plain of sandy-loam loess
96 soil (72.5% sand, 15% silt and 12.5% clay), partly covered by a biological soil crust over a thin physical crust,
97 with dry annual grasses and Shrubs.

98



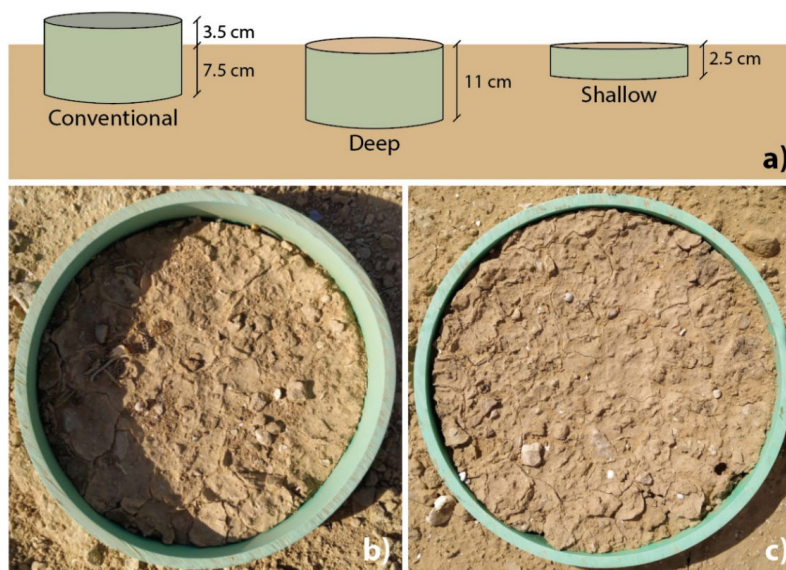
99 **2.2 Meteorological measurements**

100 Air temperature and relative humidity (100K6A1A, BetaTherm, USA) were monitored along with wind speed
101 and direction as part of an eddy-covariance system (IRGASON, Campbell Scientific Inc.). Air temperature was
102 measured at 5-second intervals and averaged over 15-minute periods. Wind speed and direction were determined
103 from high-frequency measurements of 3D wind speed taken at 20 Hz intervals, then averaged over 30-minute
104 periods and stored in a data logger (CR6, Campbell Scientific Inc.). Net radiation was measured at a height of 2.4
105 m using a 4-component net radiometer (SN-500-SS, Apogee instrument Inc, USA) at 10-second intervals,
106 averaged over 15-minute periods, and stored in a data logger (CR5000, Campbell Scientific Inc.).

107 **2.3 Soil CO₂ flux measurements**

108 We measured F_s using a non-dispersive Infrared Gas Analyzer with a range of 0-20,000 ppm and an accuracy of
109 1.5% of reading. The analyzer was connected to four automated non-steady-state chambers (LI 8100A- 104C, LI-
110 COR, Lincoln, USA). The chambers were closed on a pre-inserted collar every 30 minutes for a measurement
111 period of 60 seconds, with a 10-second dead band period to allow homogeneous air mixing within the system.
112 Each measurement started with a 90-second pre-purge and ended with a 45-second post-purge period.

113 We deployed the chambers on three types of collars (i.e., treatments): (1) The conventional type (CONV) - an 11
114 cm long collar, inserted 7.5 cm into the soil, leaving 3.5 cm of collar above the soil surface (Fig. 1); (2) The deep
115 type (DEEP) - an 11 cm long collar completely inserted into the soil, leaving the top of the collar flush with the
116 soil surface; and (3) The shallow type (SHAL) - a 2.5 cm long collar completely inserted into the soil, with the
117 top of the collar flush with the soil surface. Three collars from each type (1-3) were inserted into the soil two
118 months before measurements started. All collars had an inner diameter of 20 cm.



119 **Figure 1: a) The three types of collars used in this experiment. b) Photo of a conventional (CONV) collar. c) Photo of**
120 **a collar flashed with the soil surface, representing the DEEP and SHAL treatments.**
121



122 We collected data between May and June of the 2021 dry season. Three chambers were rotated between the collars
 123 on a near-weekly basis (periods 1-6; Table 1), ensuring that each period consisted of at least five full and
 124 representative days. The fourth chamber was placed on an additional DEEP collar for the whole experiment
 125 duration (the permanent type - PERM). The chambers were rotated in two configurations (Table 1): during periods
 126 1, 3 and 5, each chamber was set over a different treatment, e.g., in period 1, chambers were placed over collars
 127 CONV1, DEEP1, SHAL1; and during periods 2, 4 and 6, the three chambers were placed on the same treatment
 128 (SAME), e.g., in period 2, chambers were placed over collars CONV1, CONV2, CONV3.

129

Table 1. Chamber placement during the 6 measurement periods - 12/05-29/06/2021

Period	1	2	3	4	5	6
Dates	12-18/05	18-22/05 27-30/05	30/05-03/06 06-09/06	09-16/06	16-22/06	24-29/06
Analyzed days	12-16/05	19-21/05 28-29/05	31/05-02/06 07-08/06	09-14/06	17-21/06	25-29/06
Treatment and replicate	CONV1 DEEP1 SHAL1	CONV 1-3	CONV2 DEEP2 SHAL2	DEEP 1-3	CONV3 DEEP3 SHAL3	SHAL 1-3

One chamber (PERM) continuously measured soil CO₂ flux on the same collar throughout the experiment.

130 **2.4 Ancillary soil measurements**

131 The temperature profile in the soil was measured by self-made T-type thermocouples buried at depths of 0.5, 1,
 132 2, 3, 4, 5, 10, 15, 20, 30 and 50 cm. The thermocouple buried at 0.5 cm provided a proxy for the soil surface
 133 temperature. The soil heat flux was derived using the combination method with three repetitions, using a soil heat
 134 flux plate (HFT3, Campbell Scientific Inc.) buried at a depth of 5 cm. Heat storage above the plates was derived
 135 from two self-made T-type thermocouples buried at depths of 1.25 and 3.75 cm, and soil water content was
 136 measured with a time-domain reflectometer (TDR-315, Acclima, Inc., USA) installed at a depth of 3 cm. The
 137 volumetric water content of the soil was lower than 3% throughout the experiment. Temperature profile and water
 138 content data were collected at 10-second intervals, and 15-minute averages were stored in a data logger
 139 (CR1000X, Campbell Scientific Inc.) and multiplexer (AM 16/32B, Campbell Scientific Inc.). Soil heat flux data
 140 were also collected at 10-second intervals, and 15-minute averages were stored in a data logger (CR5000,
 141 Campbell Scientific Inc.).

142 **2.5 Radiometric surface temperature**

143 A 24-hour field campaign was conducted on August 17-18, 2021. During the campaign, the surface radiometric
 144 temperature of the collars was acquired hourly using a thermal infrared camera (A655sc, FLIR, Wilsonville,
 145 USA), immediately before taking F_s measurements.

146 **2.6 Data analysis**

147 To calculate F_s , a linear function was fitted to the change in CO₂ mole fraction over time for each measurement,
 148 using the software LI-COR SoilFluxPro 5.2.0 (LI-COR, Lincoln, USA). The fitting period, which usually lasted
 149 20 seconds, started after air mixing within the chamber was achieved.



150 To decipher the differences between collars, and given the limited number of chambers, we derived an “average-
151 day” for each collar type (CONV, DEEP, and SHAL). First, five full representative days from each experiment
152 period (Table 1) were analyzed. Then, for each of the four chambers, an average diel course was calculated from
153 the 5 analyzed days, resulting in 4 average days per period. All average days from all periods (4 treatments × 6
154 periods= 24 average days) were then divided into 3 groups based on collar type (6 average days per treatment),
155 and a single average day per treatment was calculated as the mean of the 6 average days. Each time point in the
156 three treatment average days consists of 30 values (6 average days × 5 days per average).

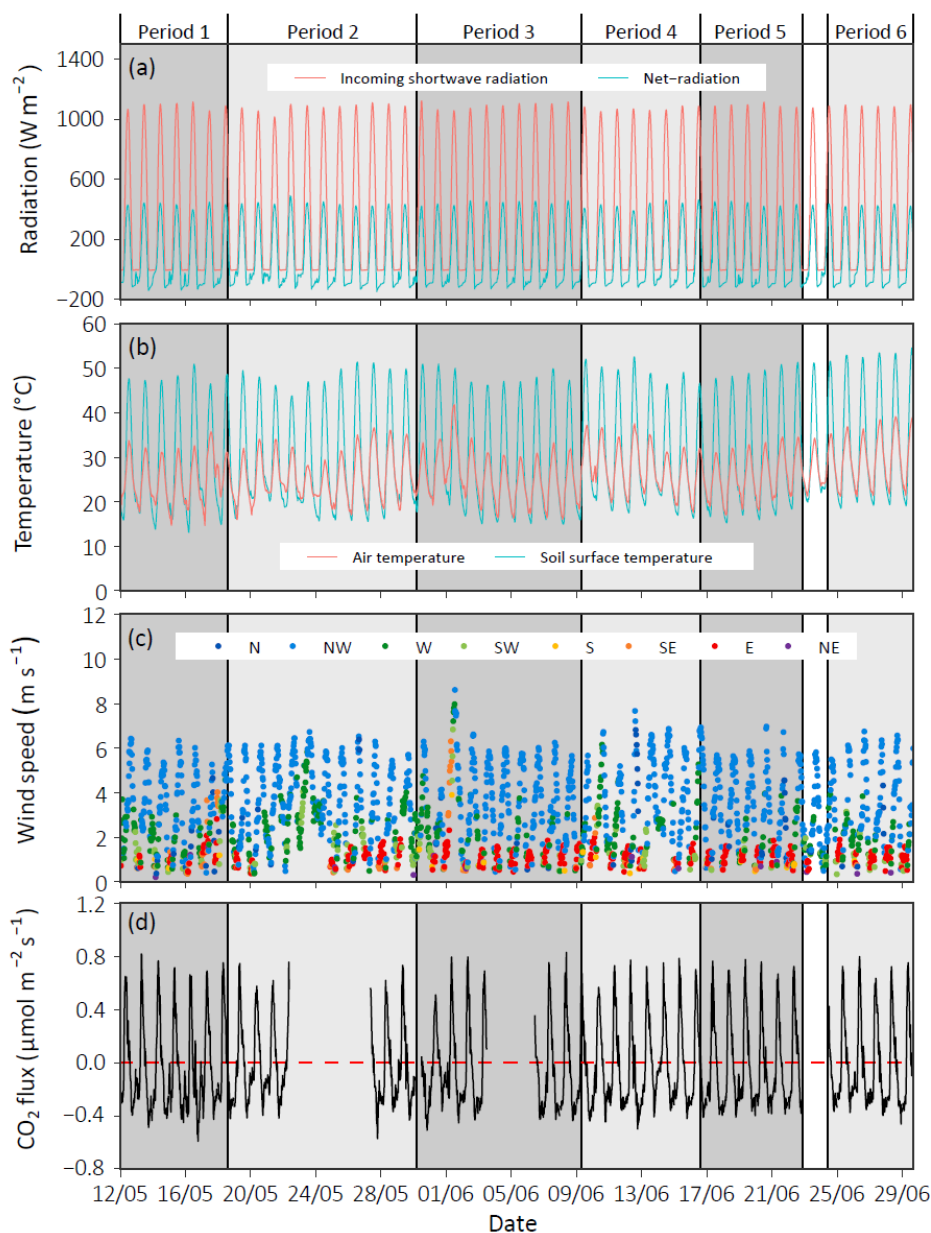
157 The differences between the treatments were tested for significance using linear mixed models (LMMs), following
158 the approach developed by Spyroglou et al. (2021). We built a statistical model Using LMMs that predicted the
159 response variable (i.e., the mean daily cycle of F_s) as a function of treatment and time as fixed factors (fixed for
160 all data points), and each collar as a subject-specific factor (random effect). This allowed us to assess the effect
161 of treatment, but also the effect of time and individual collars on F_s , while incorporating all 24-hour time series
162 into a single model. Still, this model fails to defuse the autocorrelation between data points in each time series. To
163 address this, the LMM residuals were passed through an Autoregressive Integrated Moving Average (ARIMA)
164 model and then incorporated within the LMM as errors. The predicted F_s values produced by the corrected model
165 were compared between treatments for each time interval separately using a two-tale t-test with a 95% confidence
166 interval. To avoid type I errors, the p-value was divided by the number of tests performed on each time point
167 according to the Bonferroni correction. Therefore, the corrected p-value used here is $0.05/6=0.008$. The
168 differences between the treatments were also tested by comparing peak daily and daily accumulated efflux and
169 uptake value. This was executed using one-way ANOVA and a post hoc Tukey test with a 95% confidence
170 interval. The modeling process and statistical analysis were performed using “stats”, “lme4” and “forecast”
171 packages in RStudio 4.1.1.

172 To analyze the collars surface temperature, the region of interest (ROI) for each thermal image was defined for
173 the collar’s inner surface area using FLIR ResearchIR Max 4.40.35. The surface temperature of all pixels within
174 the ROI were then exported to RStudio to calculate statistical parameters used to compare treatments. The soil
175 surface emissivity was set to 0.95 for all images (Li et al., 2013).

176 **3 Results**

177 **3.1 Meteorological and soil conditions**

178 The experiment period was characterized by clear sky days, with similar diel patterns and magnitudes of incoming
179 short-wave and net-radiation (Fig. 2). Solar noon occurred at 11:30 every day of the experiment (UTC+02:00).
180 Sunrise and sunset occurred at 04:30-05:00 and 19:00, respectively. The daily minimum and maximum air and
181 soil surface temperatures were 19.45 ± 2.3 and 34.5 ± 2.7 C° (air) and 17.7 ± 2 to 49.6 ± 2.2 C° (soil surface),
182 respectively. The mean daily range was 13.7 ± 1.0 and 31.8 ± 1.2 C°, for the air and the soil surface respectively,
183 with a slight variation between the experiment weeks. The soil surface temperature regularly dropped below air
184 temperature at night (Fig. 2B). The prevailing wind direction was NW, peaking in the afternoon at a mean speed
185 of 6.2 ± 0.2 m s⁻¹ (2 m height).



186

187 **Figure 2: Time series with half hourly data of environmental variables measured at the Wadi Mashash Experimental**
 188 **farm during the 2021 summer season. A) Incoming shortwave radiation and net radiation. B) Air and soil surface**
 189 **temperatures measured at 0.5 cm depth. C) Wind speed is color-coded according to wind direction: north (N), north-**
 190 **west (NW), west (W), south-west (SW), south (S), south-east (SE), east (E), and north-east (NE). D) The soil CO₂ flux**
 191 **measured by the permanent chamber (PHARM).**

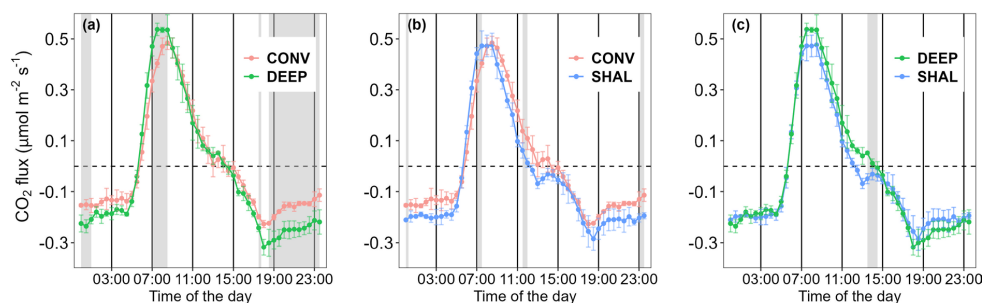
192 Soil CO₂ flux measured on the permanent collar followed a consistent diurnal pattern throughout the experiment
 193 (Fig. 2d), confirming that the weekly periods can be used to test differences between treatments. Starting from the
 194 afternoon (mean time 13:30), negative CO₂ flux (i.e., uptake; from the atmosphere to the soil) occurred, peaking,



195 on average, at a flux of $-0.4 \pm 0.04 \mu\text{mol m}^{-2} \text{s}^{-1}$ (at 18:30). Then in the early morning (06:00), the flux reversed,
 196 and positive CO_2 flux (i.e., efflux; from the soil to the atmosphere) increased sharply until 08:30, when a daily
 197 maximum of $0.71 \pm 0.08 \mu\text{mol m}^{-2} \text{s}^{-1}$ was observed. After that, efflux gradually decreased until the afternoon.

198 3.2 The effect of collar type on soil CO_2 flux

199 The daily temporal dynamic of F_s shows little variation among the different treatments. However, the rate of
 200 increasing CO_2 efflux in the early morning, measured by the CONV collars, was lower than in the other treatments,
 201 as evidenced by the curve's concave nature (Fig. 3). Consequently, the daily maximum CO_2 efflux of CONV
 202 occurred at 08:30, an hour later than in the other treatments. The SHAL collars were also different from the other
 203 treatments in the timing of CO_2 uptake onset, occurring each day between 12:00-12:30, two hours before uptake
 204 started in the other treatments (Fig. 3).



205

206 **Fig. 3.** Mean daily cycles of the soil CO_2 flux measured in the following collar types- A) The conventional (CONV) and
 207 deep (DEEP) insertion types. B) The conventional (CONV) and shallow (SHAL) types. C) The shallow (SHAL) and
 208 deep (DEEP) types. Error bars denote two standard deviations ($n=30$). Gray areas represent periods in which
 209 differences between the treatments were statistically significant ($p\text{-value} < 0.008$).

210 The LMM model, combined with time series analysis, yielded statistically significant results ($P < 0.008$) for the
 211 differences in F_s between CONV and DEEP during the morning (07:00-08:30) and the evening/night (17:30-
 212 01:00). In fact, F_s of CONV were consistently lower than in DEEP. The relative differences peaked at 06:00 and
 213 23:30, when mean daytime CO_2 efflux and nocturnal CO_2 uptake were 56 and 53% lower in the CONV than in
 214 the DEEP. F_s measured in the CONV collars were also significantly lower than SHAL, by a maximum of 41%,
 215 but for shorter periods around noon and midnight. F_s measured in the DEEP collars were only significantly
 216 different from SHAL ($P < 0.008$) from 13:30 to 14:30.

217 The mean peak daily efflux measured in the DEEP treatment differed significantly from the other two treatments
 218 ($p < 0.05$), while no statistically significant difference in peak efflux was found for SHAL and CONV (one-way
 219 ANOVA and Tukey post hoc test). The differences between the total daily amount of CO_2 emitted during the day
 220 measured in SHAL and CONV were also insignificant ($p > 0.05$; Table 2). In contrast, the total daily amounts of
 221 CO_2 uptaken by the soil in the CONV collars were significantly lower than in the SHAL and the DEEP collars
 222 (Table 2), which may lead to erroneous estimations of daily net CO_2 exchange.

223

224



Table 2. Summary of main features- the mean daily cycles of F_s

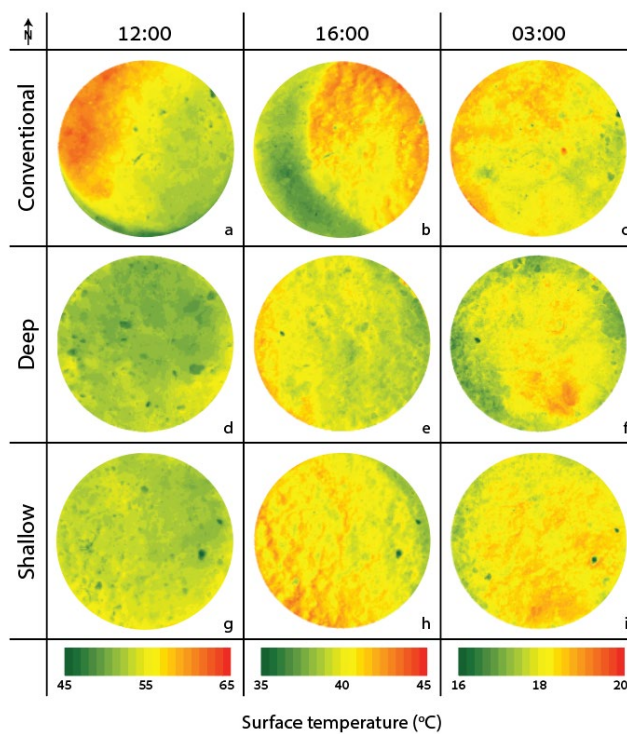
Period	Treatment	Max CO ₂ efflux	Max CO ₂ uptake	Total uptake	Total efflux
		$\mu\text{mol m}^{-2} \text{s}^{-1}$	$\mu\text{mol m}^{-2} \text{s}^{-1}$	g m^{-2}	g m^{-2}
1	CONV1	0.51±0.08	-0.28±0.04	0.43±0.077	0.29±0.04
	DEEP1	0.61±0.06	-0.38±0.05	0.54±0.05	0.39±0.06
	SHAL1	0.59±0.06	-0.38±0.06	0.57±0.10	0.32±0.05
2	CONV1	0.47±0.04	-0.26±0.03	0.30±0.05	0.33±0.04
	CONV2	0.51±0.06	-0.26±0.03	0.28±0.04	0.37±0.03
	CONV3	0.52±0.07	-0.27±0.02	0.31±0.06	0.32±0.04
3	CONV2	0.57±0.09	-0.25±0.04	0.36±0.11	0.39±0.04
	DEEP2	0.61±0.07	-0.36±0.03	0.53±0.13	0.34±0.09
	SHAL2	0.58±0.10	-0.35±0.03	0.49±0.12	0.33±0.08
4	DEEP1	0.64±0.08	-0.38±0.04	0.47±0.11	0.41±0.05
	DEEP2	0.67±0.11	-0.40±0.03	0.52±0.14	0.40±0.05
	DEEP3	0.57±0.10	-0.34±0.07	0.43±0.14	0.33±0.05
5	CONV3	0.55±0.04	-0.27±0.03	0.41±0.04	0.33±0.03
	DEEP3	0.60±0.01	-0.30±0.02	0.47±0.03	0.36±0.04
	SHAL3	0.48±0.04	-0.28±0.03	0.44±0.02	0.28±0.04
6	SHAL1	0.56±0.03	-0.32±0.01	0.46±0.11	0.34±0.01
	SHAL2	0.52±0.04	-0.28±0.03	0.37±0.08	0.28±0.03
	SHAL3	0.48±0.02	-0.27±0.02	0.35±0.09	0.29±0.03

225 Each value in the table is an average of 5 days ± one standard deviation.

226

227 3.3 The effect of collar type on the radiometric soil surface temperature

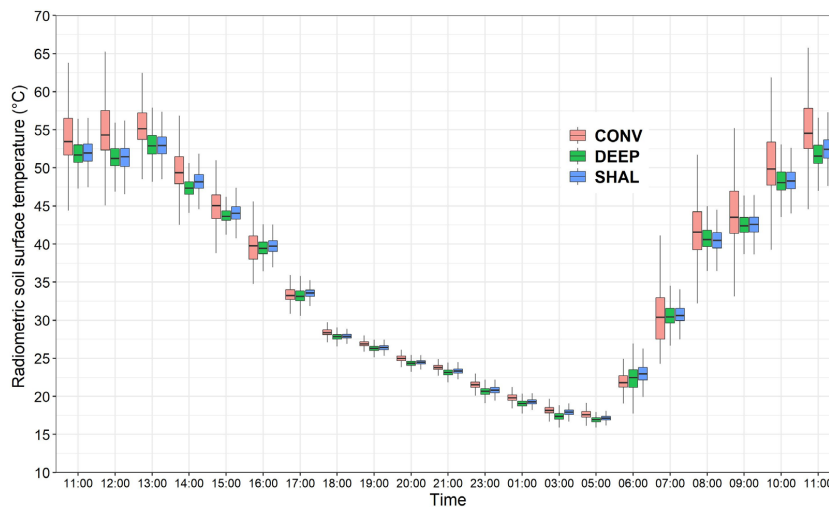
228 The mean and range of soil radiometric surface temperatures in the CONV collars were higher than in the DEEP
 229 and SHAL collars, even at midday (Fig. 4). At 16:00, the three treatments all exhibited a mean surface temperature
 230 of 40 °C, but the range of surface temperatures in the CONV collars doubled those of the other treatments. During
 231 the night, the mean surface temperature of the CONV collars was 0.5-1 °C higher than in the DEEP collars and
 232 0.5-0.9 °C higher than in the SHAL collars. After sunrise, the surface temperatures of the CONV and SHAL
 233 increased faster than in the CONV collars up to 07:00. Later, the mean surface temperature of DEEP and SHAL
 234 maintained a similar distribution over time, while the range and mean surface temperature in the CONV increased
 235 sharply (Fig. 5).



236

237 **Figure 4: Thermal images of the soil surface radiometric temperature of one collar for each treatment in example hours**
 238 **of the day. A-C) The conventional treatment. D-F) The deep treatment. G-I) The shallow collar treatment. Note that**
 239 **each hour has a different temperature range.**

240



241

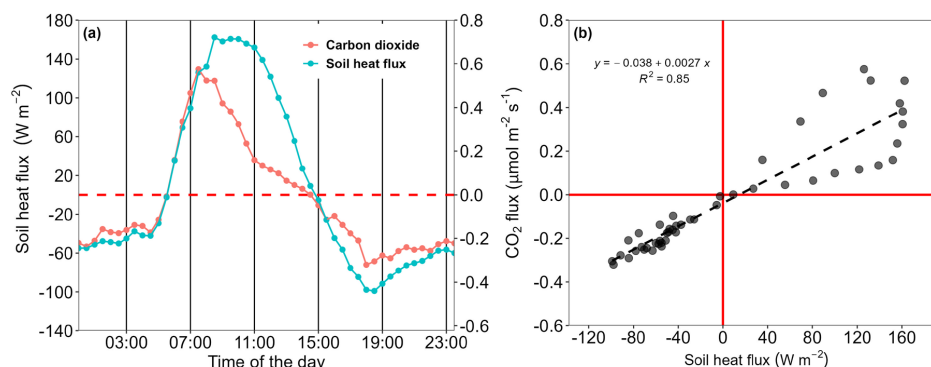
242 **Figure 5: Box plot and whiskers of the radiometric soil surface temperatures measured within the 3 types of collars on**
 243 **the 17-18/08/2021.**



244 **3.4 The effect of the soil heat flux on soil CO₂ flux**

245 Changes in soil surface temperature induced by the collar treatment significantly affected F_s . Nonetheless, F_s and
 246 soil surface temperatures were uncoupled throughout the day and therefore may not be the sole variable that
 247 explains F_s dynamics (Figs. 3 and 5). For example, while the soil surface temperature decreased throughout the
 248 night, F_s decreased until the evening (18:00) and slowly increased during the night. However, the soil surface
 249 temperature has a prime effect on the temperature profile within the soil, as well as the direction and magnitude
 250 of soil heat flux. In fact, fig. 6 shows that F_s was linearly correlated with the soil heat flux, during the night and
 251 morning efflux. Later, F_s decreased earlier than the soil heat flux, resulting in a daytime hysteresis relationship
 252 (Fig. 6b).

253



254 **Figure 6: Relationship between the mean days of F_s and the soil heat flux for period 4 (9-16/06/2021).** Note that positive
 255 F_s values indicate that the direction of the flux is from the soil to the atmosphere and vice versa for negative F_s values.
 256 Positive and negative soil heat flux values indicate the opposite directions than F_s values.

257 **4 Discussion**

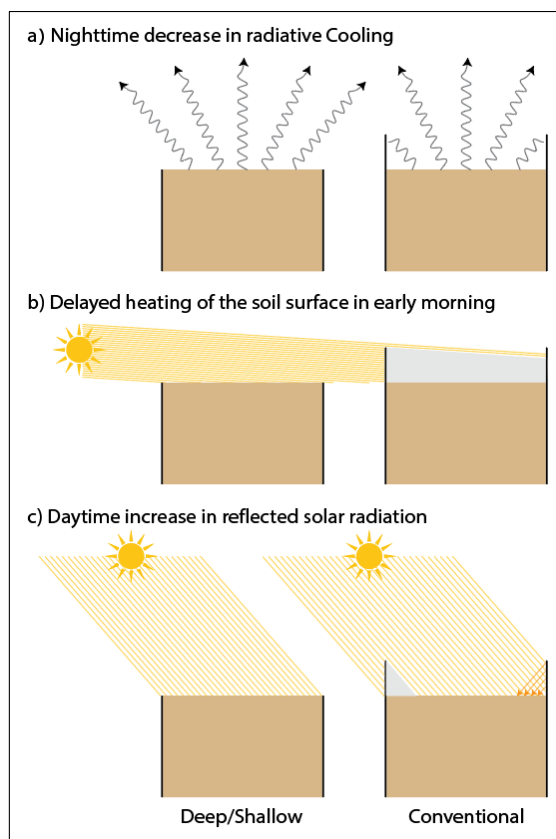
258 Our study's results indicate that in dry and bare desert soils, using collars that protrude over the soil surface
 259 (CONV) can decrease F_s . This finding is consistent with a prior global assessment that identified a negative
 260 correlation between collar height above the soil surface and mean annual soil respiration rates (Jian et al., 2020).
 261 However, while we found that protruding collars resulted in significant errors of nearly 50% in F_s (Fig. 3 and
 262 table 2), Jian et al. (2020) demonstrated that collar height leads to a much smaller bias of only ~10% in annual
 263 soil respiration rates. They explained this bias by nonuniform air mixing within the chamber system resulting
 264 from the larger system volume but did not consider the potential effect of elevated collars on soil surface
 265 temperatures. Moreover, 85% of the annual soil respiration rate values Jian et al. (2020) used were estimated
 266 based on a limited number of instantaneous CO₂ efflux measurements, which were usually performed during the
 267 daytime, and, therefore, overlook diurnal dynamics in F_s . Since F_s is not constant throughout the day in desert
 268 soils but varies between daytime efflux and nocturnal uptake (Fig. 3), a small discontinuous number of daytime
 269 measurements will fail to capture errors in flux measurements. Finally, while most studies discussing potential
 270 sources of errors in F_s measurements were conducted in conditions where the dominant flux is a result of microbial
 271 respiration, in dry desert soils F_s is primarily driven by an abiotic process governed by changes in soil temperatures
 272 (Soper et al., 2017). Therefore, errors associated with using static chambers in dry desert soils are likely related



273 to alteration of geochemical processes in the soil rather than affecting the factors that influence soil microbial
274 activity.

275 The abiotic process driving nocturnal CO₂ uptake in dry desert soils is often explained by the combined effect of
276 contraction and dissolution of gaseous CO₂ in soil water. These processes decrease gaseous CO₂ concentration in
277 the soil surface layer, forming an atmosphere-to-soil concentration gradient and CO₂ diffusion into the soil (Sagi
278 et al., 2021; Yang et al., 2020). Contraction of soil air may decrease CO₂ concentration in the soil surface layer
279 and lead to atmosphere-to-soil pressure gradient and thermal convection, which further contributes to CO₂ uptake
280 (Ganot et al., 2014). Soil temperature negatively affects both contraction and dissolution. Higher temperature
281 result in less contraction and dissolution, thus a higher CO₂ concentration in the surface air-filled soil-pores,
282 ultimately leading to a smaller soil-atmosphere CO₂ gradient, and lower F_s .

283 The elevated walls in the CONV collars limit nocturnal radiative cooling of the topsoil layer, resulting in higher
284 soil temperatures that suppress the CO₂ concentration gradient and the actual CO₂ uptake from the atmosphere
285 (Fig. 4 and fig. 7). Following sunrise, soil temperature increases in the DEEP and SHAL collars, promoting CO₂
286 expansion and outgassing from water films, rapidly increasing CO₂ efflux (Fa et al., 2016). This process is delayed
287 in the CONV collars because the surface is entirely shaded by the collar walls (Fig. 7b), resulting in a lower mean
288 temperature and a narrower overall range of surface temperatures (Fig. 5; 06:00 and Fig. 7b). As a result, CO₂
289 efflux increases at a slower rate (Fig. 3). When the sun elevation increases, solar radiation is reflected off the
290 collar walls into the measured area, increasing the radiation flux in the unshaded soil surface and, consequently,
291 increasing the mean and range of soil surface temperatures compared to the DEEP and SHAL collars (Figs. 4A-
292 B, 5 and 7). Thus, lower surface temperatures cannot explain the significantly lower CO₂ efflux measured in the
293 CONV collars between 07:00 and 08:30. Instead, it is probably related to the significantly lower total nighttime
294 CO₂ uptake, which leads to a faster depletion of soil CO₂ in the following morning (Table 2).



295

296

297

Figure 7: Conceptual model showing the effects of collar deployment on soil surface radiative heating and cooling during the night (a), early morning (b), and daytime (c).

298

299

The results of our study indicate that lateral diffusion is not a significant concern in dry, bare desert soils when the measurement period (i.e., the length of time during which the chamber is closed over the collar) is short, as demonstrated by the insignificant differences between F_s measured over the SHAL and DEEP collars. This confirms the findings of Hutchinson and Livingston, (2001). Although statistically insignificant, the mean CO_2 efflux in the SHAL collars was consistently lower than in the DEEP collars between 7:00 and 14:30 (Fig. 3 and table 2). Additionally, the flux direction measured over the SHAL collars, consistently changed from efflux (positive) to uptake (negative) earlier than in the other treatments, and earlier than the soil heat flux changed from positive to negative (Fig. 6). A change in the soil heat flux sign indicates that temperatures in the uppermost soil layer are decreasing, promoting the removal of gaseous CO_2 from the soil air phase, followed by CO_2 uptake from the atmosphere. Hence, when soil temperatures are undisturbed (e.g., by the presence of a collar), we expect the onset of CO_2 uptake to coincide with the change in soil heat flux direction (Fig. 6). The only difference between the SHAL and DEEP collars was their insertion depth (in both the collar's top end was flashed with the soil surface). Root cutting, which is often suggested as an explanation for lower F_s measured over deeper collars (Heinemeyer et al., 2011), is inapplicable when the soil is sparsely vegetated. Furthermore, our results show higher

312



313 F_s values when measured over deeply inserted collars (DEEP) then when measured over shallow collars (SHAL).
314 Potential overestimation of F_s resulting from enhanced air flow along the collar walls in the DEEP collars was
315 minimized by inserting the collars more than two months prior the measurements, a sufficiently long time to allow
316 the soil to settle around them (Hutchinson and Livingston, 2001). Lateral diffusion below the shallow collars
317 therefore remains the most probable explanation. As suggested by Healy et al. (1996), lateral movement likely
318 decreased the CO₂ concentration in the soil top layer during CO₂ efflux, decreasing the concentration gradient
319 between the soil and the chamber headspace, resulting in an underestimation of F_s . The lower soil CO₂
320 concentration beneath the SHAL collars caused the concentration gradient that drives the vertical flux to reverse
321 direction toward the soil, starting CO₂ uptake earlier than in the other treatments (fig. 3).

322 The conventionally deployed collars (CONV) underestimated the instantaneous CO₂ uptake and thus the total CO₂
323 uptake during the night (table 2). This suggests that the actual carbon sequestration by desert soils is higher than
324 previously reported. Theoretically, if F_s in dry desert soils is derived by abiotic geochemical processes, a balanced
325 net daily cycle would be expected, where nocturnal CO₂ uptake is compensated by daytime efflux. Even in alkaline
326 soils, such as the ones in our study site, where the nocturnal dissolution of CaCO₃ may sustain CO₂ uptake from
327 the atmosphere, the reverse reaction should occur when water evaporates and CaCO₃ precipitates, promoting CO₂
328 efflux and system equilibrium (Roland et al., 2013). This hypothesis was supported by Hamerlynck et al. (2013)
329 who found that a soil in the Chihuahuan Desert, USA, only serves as a minor carbon sink (0.88 g C m⁻²
330 accumulated over three months) and concluded that this contribution is insignificant to the global carbon balance.
331 Contrarily, in the Taklamakan (Yang et al., 2020) and the Gubantonggut (Xie et al., 2009) Deserts in China,
332 nocturnal CO₂ uptake led to a mean annual uptake of 7.11 and 62-622 g C m⁻², respectively. This gave rise to the
333 hypothesis that nocturnal CO₂ uptake by desert soils might explain a substantial portion of the global missing sink.
334 However, they did not provide a mechanism to explain where the carbon is stored, especially given that the
335 leaching of dissolved carbonates to groundwater is limited in space and time (Ma et al., 2014; Yang et al., 2022).
336 Either way, no conclusions can be drawn about the role desert soils play in the missing sink until a methodology
337 to measure these small fluxes is proved to be accurate. Our study shows that instantaneous F_s and F_s daily balance
338 could be significantly affected by even as small as a few centimeters difference in collar height and depth. This
339 implies that previous estimates of the carbon balance of desert ecosystems using static chambers need to be
340 carefully considered.

341 5 Summary and Conclusions

342 The drivers of abiotic soil CO₂ flux observed in dry desert soils are yet far from being understood. Further research
343 is needed to reconcile the discrepancy between the theoretical basis, which suggests a balanced daily cycle, and
344 field measurements, which often show net uptake by the soil in both diel and annual scales. Particularly, studies
345 should focus on improving our understanding of CO₂ in the soil profile in desert soils, and on allocating the
346 sources of water that are assumed to act as a solvent for CO₂ even when the soil is dry. None of these questions,
347 however, can be addressed without an accurate methodology to measure the small F_s characterizing bare desert
348 soils.

349 During a two months measurement period in the summer of 2021, the soil in the Wadi Mashash Experimental
350 farm exhibited a repetitive diel cycle of CO₂ flux that consisted of nocturnal CO₂ uptake and daytime efflux,



351 driven by a combination of physical and geochemical processes in the soil. We show here for the first time that
352 collar deployment practices significantly affect this abiotic diel cycle by altering the factors that drive F_s . Notably,
353 morning CO_2 efflux and nocturnal CO_2 uptake were underestimated when measured on conventionally inserted
354 collars because the elevated collar walls distorted the ambient surface temperature regime. We conclude that in
355 bare desert soils collars should be deployed flush with the soil surface to prevent distortion of heat exchange
356 between the soil and the atmosphere and between soil layers, two important drivers of the abiotic F_s . Lateral
357 diffusion under shallow collars may occur and affect F_s ' temporal dynamics. However, we found this to be of a
358 lesser concern in compact soils and short measurement periods. Still, in dry desert soils, the collar insertion depth
359 should exceed the depth at which the fluctuations in soil CO_2 concentration that drive F_s occur, roughly 2 cm
360 (Hamerlynck et al., 2013).

361 Deployment protocols of flux chambers should be adapted to the unique characteristics of desert soils rather than
362 follow standard procedures suitable for mesic environments. We conclude that using collars with at least 3 cm
363 length inserted flush with the soil surface will minimize measurement errors of CO_2 flux and will pave the way to
364 accurate estimates of the carbon balance of desert ecosystems.

365 **6 Code/data availability**

366 Code and data will be provided upon request.

367 **7 Author contributions**

368 **Nadav Bekin:** Conceptualization, Data curation, Formal analysis, Investigation, Methodology, Writing - original
369 draft. **Nurit Agam:** Conceptualization, Funding acquisition, Methodology, Project administration, Resources,
370 Supervision, Writing - review & editing.

371 **8 Competing interests**

372 The authors have no competing interests.

373 **9 Acknowledgments**

374 This research was supported by the Israel Science Foundation (grant number 2381/21).

375 **10 References**

- 376 Austin, A.T., Yahdjian, L., Stark, J.M., Belnap, J., Porporato, A., Norton, U., Ravetta, D.A., Schaeffer, S.M.,
377 2004. Water pulses and biogeochemical cycles in arid and semiarid ecosystems. *Oecologia* 141, 221–
378 235. <https://doi.org/10.1007/s00442-004-1519-1>
- 379 Bain, W.G., Hutyra, L., Patterson, D.C., Bright, A. V., Daube, B.C., Munger, J.W., Wofsy, S.C., 2005. Wind-
380 induced error in the measurement of soil respiration using closed dynamic chambers. *Agric. For.*
381 *Meteorol.* 131, 225–232. <https://doi.org/10.1016/j.agrformet.2005.06.004>



- 382 Baram, S., Bar-Tal, A., Gal, A., Friedman, S.P., Russo, D., 2022. The effect of static chamber base on N₂O flux
383 in drip irrigation. *Biogeosciences* 19, 3699–3711. <https://doi.org/10.5194/bg-19-3699-2022>
- 384 Brutsaert, W., 1982. *Evaporation into the Atmosphere: Theory, History, and*
385 *Applications*. Springer, Berlin.
- 386 Cable, J.M., Ogle, K., Lucas, R.W., Huxman, T.E., Loik, M.E., Smith, S.D., Tissue, D.T., Ewers, B.E., Pendall,
387 E., Welker, J.M., Charlet, T.N., Cleary, M., Griffith, A., Nowak, R.S., Rogers, M., Steltzer, H., Sullivan,
388 P.F., van Gestel, N.C., 2011. The temperature responses of soil respiration in deserts: A seven desert
389 synthesis. *Biogeochemistry* 103, 71–90. <https://doi.org/10.1007/s10533-010-9448-z>
- 390 Cable, J.M., Ogle, K., Williams, D.G., Weltzin, J.F., Huxman, T.E., 2008. Soil texture drives responses of soil
391 respiration to precipitation pulses in the sonoran desert: Implications for climate change. *Ecosystems* 11,
392 961–979. <https://doi.org/10.1007/s10021-008-9172-x>
- 393 Fa, K., Zhang, Y., Lei, G., Wu, B., Qin, S., Liu, J., Feng, W., Lai, Z., 2018. Underestimation of soil respiration in
394 a desert ecosystem. *Catena* 162, 23–28. <https://doi.org/10.1016/j.catena.2017.11.019>
- 395 Fa, K.Y., Zhang, Y.Q., Wu, B., Qin, S.G., Liu, Z., She, W.W., 2016. Patterns and possible mechanisms of soil
396 CO₂ uptake in sandy soil. *Sci. Total Environ.* 544, 587–594.
397 <https://doi.org/10.1016/j.scitotenv.2015.11.163>
- 398 Ganot, Y., Dragila, M.I., Weisbrod, N., 2014. Impact of thermal convection on CO₂ flux across the earth-
399 atmosphere boundary in high-permeability soils. *Agric. For. Meteorol.* 184, 12–24.
400 <https://doi.org/10.1016/j.agrformet.2013.09.001>
- 401 Hamerlynck, E.P., Scott, R.L., Sánchez-Cañete, E.P., Barron-Gafford, G.A., 2013. Nocturnal soil CO₂ uptake and
402 its relationship to subsurface soil and ecosystem carbon fluxes in a Chihuahuan Desert shrubland. *J.*
403 *Geophys. Res. Biogeosciences* 118, 1593–1603. <https://doi.org/10.1002/2013JG002495>
- 404 Healy, R.W., Striegl, R.G., Russell, T.F., Hutchinson, G.L., Livingston, G.P., 1996. Numerical Evaluation of
405 Static-Chamber Measurements of Soil-Atmosphere Gas Exchange: Identification of Physical Processes.
406 *Soil Sci. Soc. Am. J.* 60, 740–747. <https://doi.org/10.2136/sssaj1996.03615995006000030009x>
- 407 Heinemeyer, A., Di Bene, C., Lloyd, A.R., Tortorella, D., Baxter, R., Huntley, B., Gelsomino, A., Ineson, P.,
408 2011. Soil respiration: Implications of the plant-soil continuum and respiration chamber collar-insertion
409 depth on measurement and modelling of soil CO₂ efflux rates in three ecosystems. *Eur. J. Soil Sci.* 62,
410 82–94. <https://doi.org/10.1111/j.1365-2389.2010.01331.x>
- 411 Hillel, D., 1998. *Environmental Soil Physics*. Academic Press, San Diego, CA.
- 412 Houghton, R.A., 2007. Balancing the global carbon budget. *Annu. Rev. Earth Planet. Sci.* 35, 313–347.
413 <https://doi.org/10.1146/annurev.earth.35.031306.140057>
- 414 Hutchinson, G.L., Livingston, G.P., 2001. Vents and seals in non-steady-state chambers used for measuring gas
415 exchange between soil and the atmosphere. *Eur. J. Soil Sci.* 52, 675–682. <https://doi.org/10.1046/j.1365-2389.2001.00415.x>



- 417 Jian, J., Gough, C., Sihi, D., Hopple, A.M., Bond-Lamberty, B., 2020. Collar Properties and Measurement Time
418 Confer Minimal Bias Overall on Annual Soil Respiration Estimates in a Global Database. *J. Geophys.*
419 *Res. Biogeosciences* 125, 1–13. <https://doi.org/10.1029/2020JG006066>
- 420 Li, Z.L., Wu, H., Wang, N., Qiu, S., Sobrino, J.A., Wan, Z., Tang, B.H., Yan, G., 2013. Land surface emissivity
421 retrieval from satellite data. *Int. J. Remote Sens.* 34, 3084–3127.
422 <https://doi.org/10.1080/01431161.2012.716540>
- 423 Lopez-Canfin, C., Lázaro, R., Sánchez-Cañete, E.P., 2022. Water vapor adsorption by dry soils: A potential link
424 between the water and carbon cycles. *Sci. Total Environ.* 824.
425 <https://doi.org/10.1016/j.scitotenv.2022.153746>
- 426 Lund, C.P., Riley, W.J., Pierce, L.L., Field, C.B., 1999. The effects of chamber pressurization on soil-surface CO₂
427 flux and the implications for NEE measurements under elevated CO₂. *Glob. Chang. Biol.* 5, 269–281.
428 <https://doi.org/10.1046/j.1365-2486.1999.00218.x>
- 429 Ma, J., Liu, R., Tang, L.S., Lan, Z.D., Li, Y., 2014. A downward CO₂ flux seems to have nowhere to go.
430 *Biogeosciences* 11, 6251–6262. <https://doi.org/10.5194/bg-11-6251-2014>
- 431 Ngao, J., Longdoz, B., Perrin, D., Vincent, G., Epron, D., Le Dantec, V., Soudani, K., Aubinet, M., Willim, F.,
432 Granier, A., 2006. Cross-calibration functions for soil CO₂ efflux measurement systems. *Ann. For. Sci.*
433 63, 477–484. <https://doi.org/10.1051/forest:2006028>
- 434 Ninari, N., Berliner, P.R., 2002. The role of dew in the water and heat balance of bare loess soil in the Negev
435 Desert: Quantifying the actual dew deposition on the soil surface. *Atmos. Res.* 64, 323–334.
436 [https://doi.org/10.1016/S0169-8095\(02\)00102-3](https://doi.org/10.1016/S0169-8095(02)00102-3)
- 437 Parkin, T.B., Venterea, R.T., Hargreaves, S.K., 2012. Calculating the Detection Limits of Chamber-based Soil
438 Greenhouse Gas Flux Measurements. *J. Environ. Qual.* 41, 705–715.
439 <https://doi.org/10.2134/jeq2011.0394>
- 440 Pumpanen, J., Kolari, P., Ilvesniemi, H., Minkkinen, K., Vesala, T., Niinistö, S., Lohila, A., Larmola, T., Morero,
441 M., Pihlatie, M., Janssens, I., Yuste, J.C., Grünzweig, J.M., Reth, S., Subke, J.A., Savage, K., Kutsch,
442 W., Østreg, G., Ziegler, W., Anthoni, P., Lindroth, A., Hari, P., 2004. Comparison of different chamber
443 techniques for measuring soil CO₂ efflux. *Agric. For. Meteorol.* 123, 159–176.
444 <https://doi.org/10.1016/j.agrformet.2003.12.001>
- 445 Pumpanen, J., Longdoz, B., Kutsch, W.L., 2010. Field measurements of soil respiration: Principles and
446 constraints, potentials and limitations of different methods. *Soil Carbon Dyn. An Integr. Methodol.* 16–
447 33. <https://doi.org/10.1017/CBO9780511711794.003>
- 448 Rochette, P., Eriksen-Hamel, N.S., 2008. Chamber Measurements of Soil Nitrous Oxide Flux: Are Absolute
449 Values Reliable? *Soil Sci. Soc. Am. J.* 72, 331–342. <https://doi.org/10.2136/sssaj2007.0215>
- 450 Roland, M., Serrano-Ortiz, P., Kowalski, A.S., Goddérís, Y., Sánchez-Cañete, E.P., Ciais, P., Domingo, F.,
451 Cuezva, S., Sanchez-Moral, S., Longdoz, B., Yakir, D., Van Grieken, R., Schott, J., Cardell, C., Janssens,



- 452 I.A., 2013. Atmospheric turbulence triggers pronounced diel pattern in karst carbonate geochemistry.
453 Biogeosciences 10, 5009–5017. <https://doi.org/10.5194/bg-10-5009-2013>
- 454 Sagi, N., Zaguri, M., Hawlena, D., 2021. Soil CO₂ influx in drylands: A conceptual framework and empirical
455 examination. Soil Biol. Biochem. 156, 108209. <https://doi.org/10.1016/j.soilbio.2021.108209>
- 456 Soper, F.M., McCalley, C.K., Sparks, K., Sparks, J.P., 2017. Soil carbon dioxide emissions from the Mojave
457 desert: Isotopic evidence for a carbonate source. Geophys. Res. Lett. 44, 245–251.
458 <https://doi.org/10.1002/2016GL071198>
- 459 Spyroglou, I., Skalák, J., Balakhonova, V., Benedikty, Z., Rigas, A.G., Hejátko, J., 2021. Mixed models as a tool
460 for comparing groups of time series in plant sciences. Plants 10, 1–16.
461 <https://doi.org/10.3390/plants10020362>
- 462 Stell, E., Warner, D., Jian, J., Bond-Lamberty, B., Vargas, R., 2021. Spatial biases of information influence global
463 estimates of soil respiration: How can we improve global predictions? Glob. Chang. Biol. 27, 3923–
464 3938. <https://doi.org/10.1111/gcb.15666>
- 465 Xie, J., Li, Y., Zhai, C., Li, C., Lan, Z., 2009. CO₂ absorption by alkaline soils and its implication to the global
466 carbon cycle. Environ. Geol. 56, 953–961. <https://doi.org/10.1007/s00254-008-1197-0>
- 467 Yang, F., Huang, J., He, Q., Zheng, X., Zhou, C., Pan, H., Huo, W., Yu, H., Liu, X., Meng, L., Han, D., Ali, M.,
468 Yang, X., 2020. Impact of differences in soil temperature on the desert carbon sink. Geoderma 379,
469 114636. <https://doi.org/10.1016/j.geoderma.2020.114636>
- 470 Yang, F., Huang, J., Zheng, X., Huo, W., Zhou, C., Wang, Y., Han, D., Gao, J., Mamtimin, A., Yang, X., Sun,
471 Y., 2022. Evaluation of carbon sink in the Taklimakan Desert based on correction of abnormal negative
472 CO₂ flux of IRGASON. Sci. Total Environ. 838, 155988.
473 <https://doi.org/10.1016/j.scitotenv.2022.155988>
- 474